Temperature rise and initial shrinkage of alkali-activated fly ash cement pastes

Julia Shekhovtsova
PhD Student, Department of Civil Engineering, University of Pretoria,
Pretoria, South Africa

Maxim Kovtun
Researcher, Department of Civil Engineering, University of Pretoria,
Pretoria, South Africa

Elsabe P. Kearsley
Professor, Head of Department of Civil Engineering, University of Pretoria,
Pretoria, South Africa

This paper reports on core temperature development and initial shrinkage of fly ash cement pastes activated with sodium hydroxide solution at different concentrations during elevated-temperature curing at 60°C. The results indicate that a high sodium hydroxide concentration might result in a substantial rise in the core temperature of samples, dependent on the mould size and ratio of paste to oven volume. An increase in alkali concentration was also found to increase the initial shrinkage of the pastes during elevated-temperature curing. Excessive initial shrinkage and temperature increase might lead to the appearance of internal stresses in the pastes, which can affect the material performance.

Notation

H	initial sample height (m)
H_0	initial laser reading (μm)
H_i	laser reading at time i (μm)
H_m	depth of empty cone mould (m)
H_r	thickness of reflector (m)
H_t	distance from top of mould to reflector placed on the paste surface (m)
L_w	total mass loss (%)
m_1	mass of mould with paste before elevated-temperature curing (g)
m_2	mass of mould with sample after elevated-temperature curing (g)
m_m	mass of empty mould (g)
T_p	peak temperature (°C)
t_p	time of appearance of peak temperature after the start of elevated-temperature curing (min)

Introduction

Alkali-activated materials (geopolymers, alkali-activated fly ashes, slags) are a new type of binder that utilise industrial by-products (fly ashes and slags), kaolin, rice husk ashes, different soils and so on (Bakharev *et al.*, 1999; He *et al.*, 2013; Hounsi *et al.*, 2013; Steveson and Sagoe-Crentsil, 2005). The production of geopolymers results in lower carbon dioxide emissions, making these materials 'greener' than ordinary Portland cement (OPC) binders (McLellan *et al.*, 2011; Papa *et al.*, 2014; Turner and Collins, 2013; Van Deventer *et al.*, 2010; Yang *et al.*, 2013). Numerous studies have been devoted to alkali-activated materials (Bernal and Provis, 2014; Ismail

et al., 2013; Palomo *et al.*, 1999; Provis, 2013) and the problem of strength decreases for materials with a high alkali content is continuously raised in the literature (Criado *et al.*, 2007; Fernández-Jiménez and Palomo, 2005; Heah *et al.*, 2013; Provis, 2009; Somna *et al.*, 2011; Sukmak *et al.*, 2013; Van Jaarsveld and van Deventer, 1999). Heah *et al.* (2013) reported that the compressive strength of kaolin geopolymers decreased when a high concentration of sodium hydroxide was used, due to the excess of sodium ions (Na^+) that weakened the material structure. Sukmak *et al.* (2013) reported that an excess of alkaline activator caused precipitation at a very early stage, before the condensation process, resulting in cracks on the fly ash particles. Some correlation between zeolite formation and decreased strength in geopolymers has been reported by Provis (2009) and Criado *et al.* (2007) reported that a high zeolite content prevents the attainment of high mechanical strength. Some researchers have noticed that increasing the sodium hydroxide concentration beyond an optimum point resulted in decreased strength of geopolymer paste due to early precipitation of aluminosilicate products on unreacted fly ash spheres (Somna *et al.*, 2011), which could inhibit their activation (Fernández-Jiménez and Palomo, 2005). Van Jaarsveld and van Deventer (1999) also reported that an optimum ratio of sodium oxide/silicon dioxide or potassium oxide/silicon dioxide existed for the maximum compressive strength of fly ash based geopolymers: when this ratio is exceeded, excess alkali weakens the material structure, causing a negative impact on most physical properties. Shekhovtsova *et al.* (2014) found some correlation between strength decrease and microcrack formation in samples with high alkali dosages. There are

Advances in Cement Research
Volume 28 Issue 1

Temperature rise and initial shrinkage of
alkali-activated fly ash cement pastes
Shekhovtsova, Kovtun and Kearsley

thus multiple references to strength decreases caused by a high alkali content in the literature on fly ash geopolymers. However, it is still unclear how high alkali concentrations weaken the material structure or whether there is any other factor induced by a high alkali content that affects the compressive strength of alkali-activated materials.

It is known that the reaction of alkali activation of fly ash is exothermic (Palomo *et al.*, 1999). However, the strength development of low-calcium fly ash based geopolymers is very slow at ambient temperatures (Puertas *et al.*, 2000) and elevated-temperature curing is normally used to accelerate the alkali activation process in order to gain adequate compressive strength at early ages (Alonso and Palomo, 2001a; Škvára *et al.*, 2003; Winnefeld *et al.*, 2010). The importance of heat evolution in OPC binders is well known: a large temperature rise due to the exothermal hydration process can lead to material cracking thereafter. Many parameters affect the heat evolution of OPC binder concretes, including fly ash replacement, superplasticiser dosage (Atiş, 2002) characteristics of the cement, initial material temperature, volume of poured concrete (Tarasov *et al.*, 2010), which leads to the question of what happens to alkali-activated fly ash when it is exposed to medium–high temperatures. Numerous works on heat release measurements of different alkali-activated systems have been conducted (Alonso and Palomo, 2001b; Brough and Atkinson, 2002; Chithiraputhiran and Neithalath, 2013; Fernández-Jiménez and Puertas, 1997; Muñiz-Villareal *et al.*, 2011; Palomo *et al.*, 1999; Zhang *et al.*, 2012). Zhang *et al.* (2013) reported that the heat release rate of metakaolin geopolymers increased monotonically with increasing sodium hydroxide concentration. However, even if the amount of heat released during alkali activation is known, the heat might dissipate into the surroundings or increase the temperature of the sample during elevated-temperature curing. Obviously, a large increase in temperature can damage the microstructure of the material and, as a result, can have an impact on its compressive strength and other properties. Temperatures widely used for alkali activation are as high as 60–80°C, which probably would not cause damage of the microstructure of alkali-activated fly ash. The cumulative heat from an oven combined with the internal heat from the alkali activation process might lead to a substantial rise of sample temperature and affect the newly formed material microstructure. After a review of the literature, no studies were found on how the heat released during the alkali activation process affects the core temperature development inside alkali-activated fly ash samples during elevated-temperature curing.

This work provides data on the core temperature development of sodium hydroxide activated fly ash pastes at 60°C temperature curing. The literature shows that different researchers used moulds of various sizes made from different materials to produce samples of alkali-activated pastes and mortars (Bakharev, 2005; Chindaprasirt *et al.*, 2009; Criado *et al.*,

2012; Duxson *et al.*, 2007; Ghosh and Ghosh, 2012; Görhan and Kürklü, 2014; Lemougna *et al.*, 2014; Somna *et al.*, 2011). In the work reported here, the effect of mould size and material on temperature development in the core of alkali-activated fly ash cement paste samples was investigated.

The alkali activation reaction of fly ash during elevated-temperature curing is assumed to be accompanied by volume changes due to chemical reactions and water evaporation, which can possibly lead to the appearance of internal stresses and microcracks. Various studies have investigated the shrinkage performance of different alkali-activated systems (Atiş *et al.*, 2009; Najafi Kani and Allahverdi, 2011; Ridtirud *et al.*, 2011), but most were performed on hardened materials and basically demonstrated only drying shrinkage. Initial shrinkage, however, occurs immediately after casting and during elevated-temperature curing and this might be another reason for internal stresses and performance loss of alkali-activated fly ash cement pastes. In situ measurements of the initial shrinkage of alkali-activated fly ash cement pastes during elevated-temperature curing were performed in this study utilising the shrinkage cone method (Eppers and Müller, 2010). This investigation will therefore add valuable knowledge to alkali-activated fly ash systems and will improve understanding of the processes the material experiences during elevated-temperature curing.

Experimental setup

Materials
The fly ash used for this investigation was classified as having more than 80% of particles with a particle size of less than 45 μm and with a density of 2200 kg/m³. It was mainly amorphous with inclusions of crystalline quartz and mullite. The chemical composition of the fly ash is presented in Table 1.

Sodium hydroxide flakes (98·5% purity) were dissolved in distilled water to obtain activator solutions, which were cooled to room temperature before mixing. The sodium hydroxide

Constituent	Content: wt%
Silicon dioxide (SiO_2)	55·8
Titanium dioxide (TiO_2)	1·6
Aluminium oxide (Al_2O_3)	30·3
Iron oxide (Fe_2O_3)	3·9
Magnesium oxide (MgO)	1·1
Calcium oxide (CaO)	4·1
Sodium oxide (Na_2O)	0·2
Potassium oxide (K_2O)	0·8
Phosphorus pentoxide (P_2O_5)	0·4
Loss on ignition	0·9

Table 1. Chemical composition of fly ash

Advances in Cement Research
Volume 28 Issue 1

Temperature rise and initial shrinkage of
alkali-activated fly ash cement pastes
Shekhovtsova, Kovtun and Kearsley

content of the alkali-activated fly ash cement pastes was calculated as the sodium oxide percentage of fly ash mass (3%, 6%, 9%, 12% and 15%).

Mix designs and preparation

Samples of alkali-activated fly ash cement pastes were prepared by mixing fly ash with activator solution in a pan mixer for 4 min. The paste was transferred into moulds, vibrated for an appropriate time to remove air and then cured in an oven. The total amount of water was calculated to include both the amount of water necessary to produce sodium hydroxide (solid/flake) and distilled water added to produce alkaline solution. Binder solids were calculated as the sum of fly ash mass and sodium oxide. The water to binder solids ratio (w/s) was chosen to be as low as possible, and was kept constant at 0·2. Details of the mix designs and curing conditions are shown in Table 2.

Test methods

Compressive strength

Each mixture was cast into a plastic mould according to EN 196-1 (BSI, 2005). After elevated-temperature curing, paste samples were demoulded and stored at $25 \pm 2°C$ and $65 \pm 5\%$ relative humidity until testing. The compressive strength of the alkali-activated fly ash cement pastes was tested according to EN 196-1 (BSI, 2005). The test results reported here are the arithmetic means of six compressive strength values.

Temperature development

During the first part of the temperature development test, alkali-activated fly ash cement pastes with different sodium oxide contents were cast into a set of six plastic moulds according to EN 196-1 (BSI, 2005). The total paste volume was 4·6 l. The pastes with different sodium oxide contents were cured separately. Moulds were placed in an oven at 60°C immediately after casting. T-type thermocouples were embedded into the cores of moulds during casting and two thermocouples measured the temperature in the oven. Temperature development in the sample cores was recorded at 1 min

intervals for the 24 h of elevated-temperature curing using a datalogger (Graphtec, Japan).

In the second part of the test, moulds of different sizes, made of metal and plastic were used. Alkali-activated fly ash cement pastes with 9%, 12% and 15% sodium oxide were studied. Core temperature development of the pastes with 3% and 6% sodium oxide was not investigated due to the results obtained in the first part of the test. Each of the three pastes was cast into a set of plastic and metal moulds (one of each) – 150 mm and 100 mm cubes and $40 \times 40 \times 160$ mm prisms. The total volume of each mix was 10·2 l. K-type thermocouples were placed in the core of each mould. All six moulds for each paste sample were placed in an oven at 60°C and the temperature development in sample cores was recorded for 24 h.

The oven used in this work (not equipped with a cooling system) had a net volume of 202·5 l. The ratio between paste volume and oven volume was constant at about 0·023 and 0·050 for the first and second parts of the experiment respectively.

Initial shrinkage

The alkali-activated fly ash cement pastes were studied in situ for volume changes during elevated-temperature curing in the oven. The shrinkage cone method for measuring shrinkage (Eppers and Müller, 2010) was adapted to measure volume changes of the alkali-activated fly ash cement pastes during the 24 h 60°C curing. A Micro Epsilon optoNCDT 1700 laser optical sensor with a measuring range of 2 mm was used. All components of the measuring equipment were preheated to 60°C before the test. The raw materials (fly ash and sodium hydroxide solution) were kept in a controlled-environment room ($25 \pm 2°C$ and $65 \pm 5\%$ relative humidity) for at least 24 h before the test.

Alkali-activated fly ash cement paste was cast into a cone-shaped aluminium mould that was lined with a removable plastic cone to prevent direct contact between the metallic surface and the paste, which could result in a reaction between

Paste	Sodium oxide concentration: %	w/s	Curing temperature: °C	Curing duration: h	Materials content: kg/m³		
					Fly ash	Sodium hydroxide	Water
Na3	3	0·20	60	24	1544	60	305
Na6	6	0·20	60	24	1527	118	297
Na9	9	0·20	60	24	1500	174	288
Na12	12	0·20	60	24	1469	228	278
Na15	15	0·20	60	24	1438	278	268

Table 2. Mix designs and curing conditions of alkali-activated fly ash cement pastes

Advances in Cement Research
Volume 28 Issue 1

Temperature rise and initial shrinkage of
alkali-activated fly ash cement pastes
Shekhovtsova, Kovtun and Kearsley

the alkali and aluminium of the mould. The plastic cone also ensured that adhesion of the alkali-activated fly ash cement paste to the metal surface would not influence the readings. A vibrating table was used for compaction. After compaction, the mould with paste was weighed (m_1). A reflector made out of light white plastic (to prevent its sinking into the fresh sample due to gravity) was embedded onto the paste surface. The initial height of the sample, H, was calculated from

1. $$H = H_m - H_t - H_r$$

in which H_m is the depth of the empty cone mould (m), H_t is the distance from the top of the mould to the reflector placed on the paste surface (m) and H_r is the thickness of the reflector (m). The initial height was used as the reference length for calculating the initial shrinkage.

The mould with paste was placed into the oven underneath the sensor so that the laser beam was reflected by the plastic disc. The laser sensor was adjusted to have a maximum range and measurements were started as soon as the oven was closed. The whole process from adding activator solution to the fly ash to the first displacement measurement took 5–7 min. The relative displacement was recorded by the datalogger at 10 s intervals for 24 h.

After elevated-temperature curing, the mould with paste was weighed once again (m_2) and the total mass loss was calculated as a percentage from

2. $$L_w = \frac{m_1 - m_2}{m_1 - m_m} 100$$

where m_1 is the mass of the mould with paste before elevated-temperature curing (g), m_2 is the mass of the mould with sample after elevated-temperature curing (g) and m_m is the mass of the empty mould (g).

Initial shrinkage of the sample was calculated according to

3. $$\text{Initial shrinkage} = \frac{H_i - H_0}{H}$$

where H_i is the laser reading at time i (μm), H_0 is the initial laser reading (μm) and H is the initial height of the sample (m), calculated according to Equation 1.

Results and discussion

Preliminary tests

The average compressive strengths and standard deviations (error bars) of the alkali-activated fly ash cement pastes with different sodium oxide contents are shown in Figure 1. The figure shows that the compressive strength of the pastes was
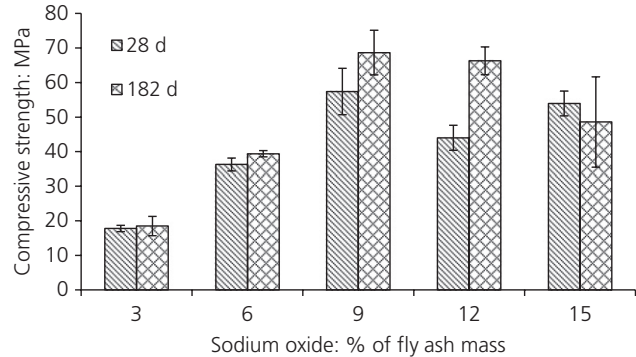

Figure 1. Effect of sodium oxide content on the compressive strength development of alkali-activated fly ash cement paste

strongly affected by sodium oxide content. An increase in sodium oxide up to 9% of fly ash mass led to an increase in compressive strength, but a further increase resulted in a decreased compressive strength. These strength results are in agreement with previous research (Shekhovtsova *et al.*, 2014). The strength decrease phenomenon was an incitement to investigate the processes occurring during elevated-temperature curing of alkali-activated fly ash cement pastes.

Temperature development

The effect of alkali concentration (sodium oxide content) on the core temperature development of the alkali-activated fly ash cement pastes during elevated-temperature curing at 60°C (the first part of the test) is shown in Figure 2.

Figure 2 clearly shows that temperature inside the sample cores increased with an increase in sodium oxide content. The core temperature of sample Na3 did not differ from the oven temperature, being constant at about 60°C throughout the test. The maximum temperatures of pastes Na6, Na9, Na12 and Na15 were 62·8°C, 68·3°C, 71·3°C and 68·2°C respectively. The time of appearance of the maximum temperature was also affected by sodium oxide content: the peak temperatures for pastes Na6, Na9, Na12 and Na15 were observed after 8·7 h, 8·9 h, 12·2 h and 15·0 h respectively. Thus the alkali activation reaction is delayed with an increase in sodium hydroxide concentration, but notably a 9% sodium oxide concentration (Na9) did not delay the activation process when compared with a 6% concentration (Na6). Alonso and Palomo (2001a) reported a lower rate of polymer formation with an increase in activator concentration. They noted that high activator concentrations produce a high pH in the liquid phase and anionic forms of silicate are more favoured, delaying polymerisation. Another observation from Figure 2 is that the pastes with lower alkali contents had narrower temperature humps than those of samples Na12 and Na15. Thus, pastes with high alkali contents were exposed to temperatures higher than 60°C for longer than the other pastes, which should affected their microstructure.

Advances in Cement Research
Volume 28 Issue 1

**Temperature rise and initial shrinkage of
alkali-activated fly ash cement pastes**
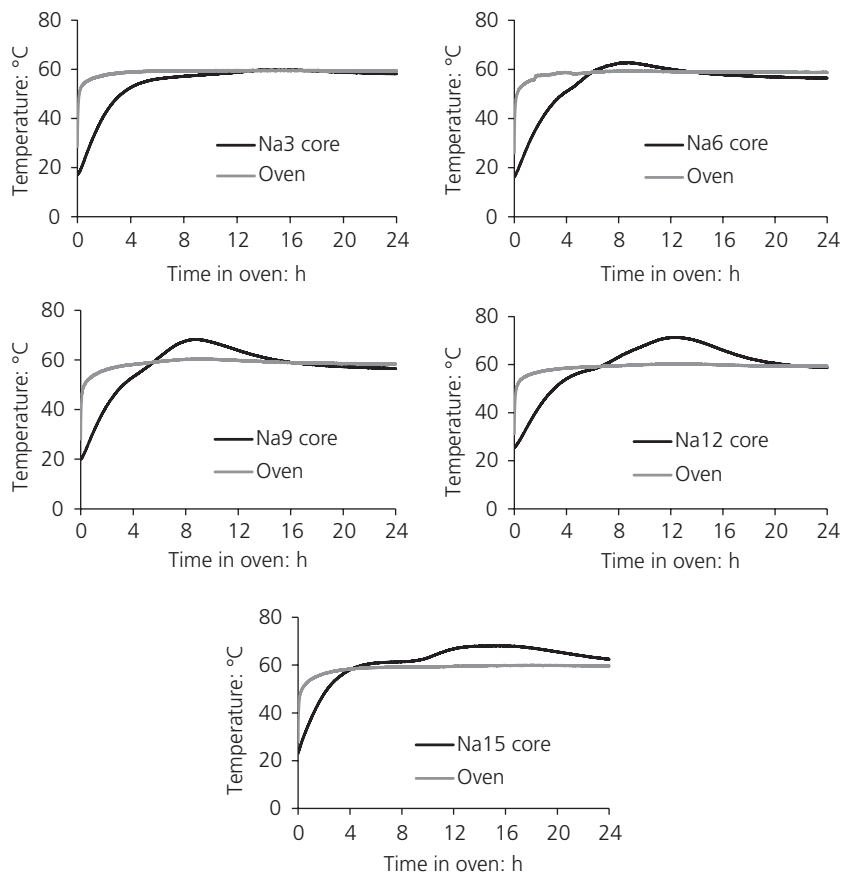Shekhovtsova, Kovtun and Kearsley

Figure 2. Core temperature development in alkali-activated fly
ash cement pastes with different sodium oxide contents during
elevated-temperature curing

Results from the second part of the temperature development test for alkali-activated fly ash cement pastes with 9%, 12% and 15% sodium oxide are shown in Figure 3. Table 3 lists the peak temperatures (T_p), the times of the appearance of peak temperature after the start of elevated-temperature curing (t_p) and the maximum temperature differences (D_{max}) between the sample core and the oven.

Several trends can be observed from Figure 3. The first trend is that the maximum core temperature was higher when the pastes were cured in plastic moulds rather than metal moulds regardless of the sodium oxide content of the pastes. The difference in maximum temperature became more prominent with an increase in the mould (sample) size. The trend can be explained by the differences in thermal conductivity properties of the mould materials (Table 4). Plastic moulds are less conductive, providing more insulation and thus preserving the heat emitted during the alkali activation process more effectively than metal moulds. Hence peak temperatures are higher in plastic moulds. This effect must be taken into account because excessive heat can damage the paste microstructure or it can

be effectively used for self-curing of alkali-activated fly ash cements, thus decreasing the curing temperature/energy consumption required during elevated-temperature curing.

The second trend is the time of appearance of the peak temperature. For the prisms and the 100 mm cube moulds, the peak appeared earlier for plastic moulds compared with metal moulds. The reverse can be seen for the case of 150 mm cube moulds. The difference in the trend between the different mould sizes is again governed by the thermal conductivity of the mould materials. In the case of the prisms and 100 mm moulds, plastic preserves the heat emitted during alkali activation, which accelerates the process, and the temperature inside the samples thus reaches the maximum value earlier in comparison with metal moulds. As mentioned, the reverse pattern can be seen for the 150 mm moulds. Before intensive alkali activation takes place, a certain amount of energy must be transferred to activate the system, and this activation energy increases with an increase in sample size. At the initial stage, compared with the metal moulds, the plastic moulds decrease the energy flux transferred from the oven environment to the
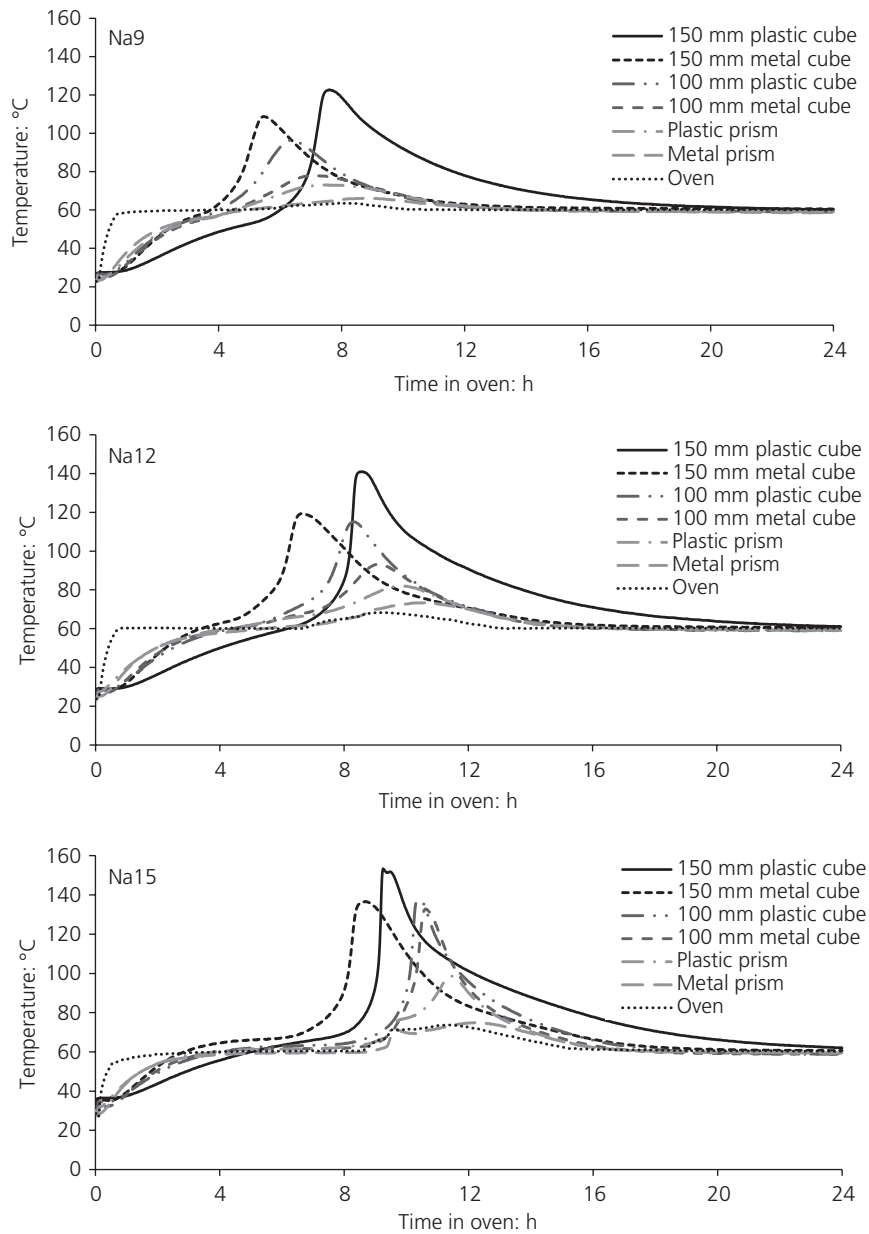
Advances in Cement Research
Volume 28 Issue 1

Temperature rise and initial shrinkage of
alkali-activated fly ash cement pastes
Shekhovtsova, Kovtun and Kearsley

Figure 3. Influence of mould size and material on the
temperature profiles of alkali-activated fly ash cement pastes with
different sodium oxide contents during elevated-temperature
curing

paste sample. This factor does not play a crucial role in the
case of prisms and 100 mm cube moulds because the ratio of
the open area (top of moulds) to the total volume is much
higher in comparison with the 150 mm moulds. The trend is
therefore influenced by both mould size and material. It is
very important to note that the time of appearance of the peak
temperature is affected by alkali concentration. The time of
maximum temperature appearance increases with an increase
in alkali concentration from 9% to 15% sodium oxide, which is

in good correlation with the results of Alonso and Palomo
(2001a). This was found to be the case for all types of moulds,
regardless of their size or material. Therefore, an increased
alkali content delays the alkali activation process.

The third trend from Figure 3 is that the maximum core tem-
perature inside the paste samples increased with an increase
in sample size and alkali content. The lowest peak temperature
corresponded to the metal prism moulds, with values of

Advances in Cement Research
Volume 28 Issue 1

Temperature rise and initial shrinkage of
alkali-activated fly ash cement pastes
Shekhovtsova, Kovtun and Kearsley

Mould/oven	Na9			Na12			Na15		
	T_p: °C	t_p: min	D_{max}: °C	T_p: °C	t_p: min	D_{max}: °C	T_p: °C	t_p: min	D_{max}: °C
150 mm metal cube	108·7	327	47·9	119·3	397	58·9	136·7	521	74·6
150 mm plastic cube	122·7	455	59·0	141·0	515	72·7	153·4	555	83·0
100 mm metal cube	78·0	422	15·1	93·2	543	24·9	132·9	637	60·5
100 mm plastic cube	96·3	378	33·9	115·0	496	48·6	137·1	621	65·0
Metal prism	66·2	528	3·9	73·4	620	7·2	74·9	731	3·4
Plastic prism	73·1	447	10·1	82·1	587	14·4	98·7	686	27·0
Oven	63·7	473	—	68·3	541	—	71·7	683	—

Table 3. Maximum temperature (T_p), time of appearance of maximum temperature (t_p) and maximum temperature difference (D_{max}) between sample core and oven

Material	Density: kg/m^3	Specific heat capacity: J/(kg.K)	Thermal conductivity: W/(m.K)	Thermal diffusivity: 10^{-6} m^2/s
Metal	7850	452	40	11·27
Plastic	1160	1700	0·28	0·14

Table 4. Mould material properties

66·2°C, 73·4°C and 74·9°C for pastes Na9, Na12 and Na15 respectively. For the 150 mm plastic cube moulds, the temperatures for Na9, Na12 and Na15 reached 122·7°C, 141·0°C and 153·4°C respectively. The significantly increased amount of heat released during the alkali activation process by the pastes with alkali content higher than 9% sodium oxide can be seen not only in the maximum temperatures reached in the paste samples but also by the temperature developed in the oven during elevated-temperature curing. The temperature inside the oven changed for a period of time due to the heat emitted, reaching peaks of 63°C, 68°C and 72°C respectively for Na9, Na12 and Na15. This is because the ratio between paste volume and oven volume was higher than in the first part of the temperature development test and the oven was not equipped with a cooling device.

High temperatures attained in a sample core lead to significant temperature differences between the sample core and the oven (Table 3), meaning that free water will boil. This boiling water will produce vapour, resulting in a build-up of pressure inside the material microstructure causing internal stresses and thus leading to possible loss in the mechanical performance of the alkali-activated fly ash cement pastes due to the formation of microstructural defects such as microcracks as observed in previous research (Shekhovtsova et al., 2014).

In general, the temperature difference between sample and oven was higher for the larger moulds made out of plastic, and increased with an increase in alkali content (Table 3). Even assuming that the surface temperature of the sample is the same as the oven temperature at any time, exact values of the stress induced by the temperature differences (Table 3) could not be calculated due to lack of data regarding the thermal expansion coefficient and elastic modulus of the alkali-activated fly ash cement pastes. Notably though, an alkali content higher than 9% sodium oxide caused considerably higher temperature differences between the sample core and oven. The internal stresses due to such temperature differences might be higher than the pastes can withstand, especially taking into account the slower polymerisation process (Alonso and Palomo, 2001a) responsible for strength development, leading to the formation of microcracks and thus loss of material performance (Shekhovtsova et al., 2014).

The temperature development test showed that alkali-activated fly ash cement pastes may experience a significant rise in core temperature, which is dependent on the ratio of paste volume to oven volume, mould size, alkali concentration and mould material. Researchers should thus take into account possible temperature increases in sample cores and in curing ovens as excessive temperature can affect material performance.

Initial shrinkage

Shrinkage strains might also lead to crack formation, and so an in situ evaluation of volume changes during elevated-temperature curing was performed for the alkali-activated fly ash cement pastes with different sodium oxide contents.

In this test, initial shrinkage does not necessary represent the amount of water evaporated during elevated-temperature

Advances in Cement Research
Volume 28 Issue 1

Temperature rise and initial shrinkage of
alkali-activated fly ash cement pastes
Shekhovtsova, Kovtun and Kearsley

curing because, along with volume changes due to water evap-
oration, chemical shrinkage and thermal movements are also
present. The initial shrinkage of the alkali-activated fly ash
cement pastes during elevated-temperature curing at 60°C is
shown in Figure 4, where each curve represents an average of
two measurements.

Figure 4 shows that shrinkage during the first 24 h of elevated-
temperature curing strongly depended on sodium oxide content.
The maximum initial shrinkage of paste Na3 was almost
3300 µε, whereas Na6, Na 9, Na12 and Na15 showed initial
shrinkages of 3800, 4300, 4700 and 5200 µε respectively. As
shown in Figure 5, there is a linear relationship between sodium
oxide content and maximum initial shrinkage, with a higher
sodium oxide content resulting in higher initial shrinkage. The
figure also shows that the maximum shrinkage rate is also a
function of sodium oxide content, decreasing with sodium oxide
content increasing from 3% to 15% of fly ash mass.

The mass loss during elevated-temperature curing for mixtures
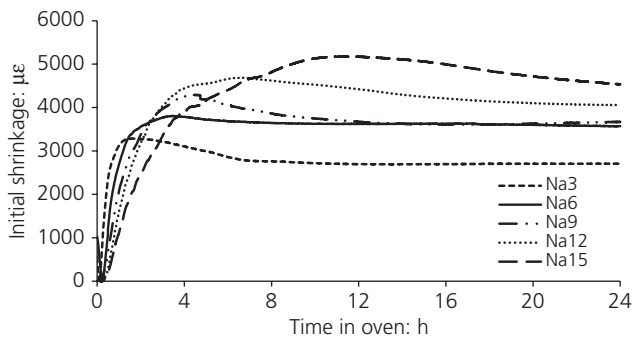with different sodium oxide concentrations is shown as a

Figure 4. Initial shrinkage of alkali-activated fly ash cement pastes
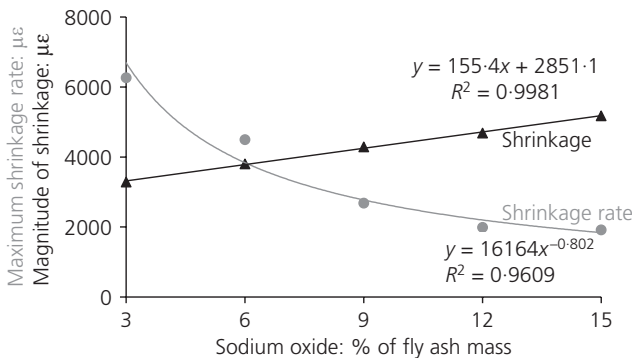with different sodium oxide contents during elevated-temperature
curing at 60°C for 24 h

Figure 5. Maximum shrinkage rate and shrinkage magnitude
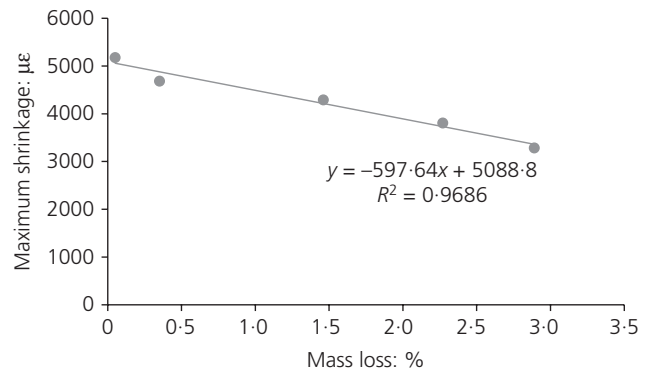versus sodium oxide content for alkali-activated fly ash cement
pastes

Figure 6. Mass loss versus maximum shrinkage for alkali-activated
fly ash cement pastes

function of maximum shrinkage in Figure 6: samples that
experienced more mass loss showed less shrinkage. It seems
that the dominating factor affecting initial shrinkage is chemi-
cal in nature. For example, sample Na3 did not produce much
reaction product (Shekhovtsova *et al.*, 2014) and the major
part of its initial shrinkage can be related to evaporated water.
In contrast, Na15 did not lose any mass during elevated-temp-
erature curing, but it did have the highest shrinkage value; this
is because more fly ash particles were dissolved in the high
alkaline solution, causing chemical contraction.

Conclusions
The following conclusions can be drawn from the results
obtained in this study.

■ Oven temperature can be affected by the heat released
during the alkali activation process if the oven is not
equipped with a cooling system and the ratio of paste
volume to oven volume exceeds a certain value.
■ The core temperature of alkali-activated fly ash cement
pastes increases significantly with increases in sodium
oxide content and mould size. The mould material also
influences paste core temperature.
■ An excessive amount of sodium oxide not only inhibits the
alkali activation process, which can be seen in the delayed
core temperature development shown in this study, but also
increases internal stresses induced by the rise in sample
core temperature and the initial shrinkage of the alkali-
activated fly ash cement pastes. These internal stresses can
weaken the structure of the material and result in a
decrease in compressive strength, as observed by many
researchers when alkali concentration exceeded a certain
threshold. The magnitude of internal stresses significantly
increases for sodium oxide contents higher than 9% of fly
ash mass.

The results of this research show that more attention should be
paid to the conditions and processes occurring during

Advances in Cement Research
Volume 28 Issue 1

Temperature rise and initial shrinkage of
alkali-activated fly ash cement pastes
Shekhovtsova, Kovtun and Kearsley

elevated-temperature curing of alkali-activated materials. Higher than intended temperatures might lead to unexpected results and could be the reason for material performance loss. Further research should be carried out to investigate the initial shrinkage mechanism and the processes occurring during elevated-temperature curing of alkali-activated materials.

REFERENCES

Alonso S and Palomo A (2001a) Alkaline activation of metakaoline and calcium hydroxide mixtures: influence of temperature, activator concentration and solids ratio. *Materials Letters* **47(1–2)**: 55–62.

Alonso S and Palomo A (2001b) Calorimetric study of alkaline activation of calcium hydroxide-metakaoline solid mixtures. *Cement and Concrete Research* **31(1)**: 25–30.

Atiş CD (2002) Heat evolution of high-volume fly ash concrete. *Cement and Concrete Research* **32(5)**: 751–756.

Atiş CD, Bilim C, Çelik Ö and Karahan O (2009) Influence of activator on the strength and drying shrinkage of alkali-activated slag mortar. *Construction and Building Materials* **23(1)**: 548–555.

Bakharev T (2005) Durability of geopolymer material in sodium and magnesium sulfate solutions. *Cement and Concrete Research* **35(6)**: 1233–1246.

Bakharev T, Sanjayan JG and Cheng YB (1999) Alkali activation of Australian slag cements. *Cement and Concrete Research* **29(1)**: 113–120.

Bernal SA and Provis JL (2014) Durability of alkali-activated materials: progress and perspectives. *Journal of the American Ceramic Society* **97(4)**: 997–1008.

Brough AR and Atkinson A (2002) Sodium silicate-based, alkali-activated slag mortars Part 1. Strength, hydration and microstructure. *Cement and Concrete Research* **32(6)**: 865–879.

BSI (2005) BS EN 196-1:2005: Methods of testing cement – part 1: determination of strength. BSI, London, UK.

Chindaprasirt P, Jaturapitakkul C, Chalee W and Rattanasak U (2009) Comparative study on the characteristics of fly ash and bottom ash geopolymers. *Waste Management* **29(2)**: 539–543.

Chithiraputhiran S and Neithalath N (2013) Isothermal reaction kinetics and temperature dependence of alkali activation of slag, fly ash and their blends. *Construction and Building Materials* **45**: 233–242.

Criado M, Fernández-Jiménez A, de la Torre AG, Aranda MAG and Palomo A (2007) An XRD study of the effect of the SiO_2/Na_2O ratio on the alkali activation of fly ash. *Cement and Concrete Research* **37(5)**: 671–679.

Criado M, Fernández-Jiménez A, Sobrados I, Palomo A and Sanz J (2012) Effect of relative humidity on the reaction products of alkali activated fly ash. *Journal of the European Ceramic Society* **32(11)**: 2799–2807.

Duxson P, Mallicoat SW, Lukey GC, Kriven WM and van Deventer JSJ (2007) The effect of alkali and Si/Al ratio on the development of mechanical properties of metakaolin-based geopolymers. *Colloids and Surfaces A: Physiochemical and Engineering Aspects* **292(1)**: 8–20.

Eppers S and Müller C (2010) The shrinkage cone method for measuring the autogenous shrinkage – an alternative to the corrugated tube method. *Proceedings of International RILEM Conference on Use of Superabsorbent Polymers and Other New Additives in Concrete, Lyngby, Denmark*, pp. 67–76.

Fernández-Jiménez A and Palomo A (2005) Composition and microstructure of alkali-activated fly ash. Effect of the activator. *Cement and Concrete Research* **35(10)**: 1984–1992.

Fernández-Jiménez A and Puertas F (1997) Alkali-activated slag cements: kinetic studies. *Cement and Concrete Research* **27(3)**: 359–368.

Ghosh K and Ghosh P (2012) Effect of synthesizing parameters on compressive strength of fly ash based geopolymer paste. *International Journal of Structural and Civil Engineering* **1(8)**: 1–11.

Görhan G and Kürklü G (2014) The influence of the NaOH solution on the properties of the fly ash-based geopolymer mortar cured at different temperatures. *Composites: Part B* **58**: 371–377.

He J, Jie Y, Zhang J, Yu Y and Zhang G (2013) Synthesis and characterization of red mud and rice husk ash-based geopolymer composites. *Cement and Concrete Composites* **37**: 108–118.

Heah CY, Kamarudin H, Mustafa Al Bakri AM et al. (2013) Kaolin-based geopolymers with various NaOH concentrations. *International Journal of Minerals, Metallurgy and Materials* **20(3)**: 313–322.

Hounsi AD, Lecomte-Nana GL, Djétéli G and Blanchart P (2013) Kaolin-based geopolymers: effect of mechanical activation and curing process. *Construction and Building Materials* **42**: 105–113.

Ismail I, Bernal SA, Provis JL et al. (2013) Influence of fly ash on the water and chloride permeability of alkali-activated slag mortars and concretes. *Construction and Building Materials* **48**: 1187–1201.

Lemougna PN, Chinje Melo UF, Delplancke MP and Rahier H (2014) Influence of the chemical and mineralogical composition on the reactivity of volcanic ashes during alkali activation. *Ceramics International* **40(1)**: 811–820.

McLellan BC, Williams RP, Lay J, van Riessen A and Corder GD (2011) Cost and carbon emissions for geopolymer pastes in comparison to ordinary Portland cement. *Journal of Cleaner Production* **19(9–10)**: 1080–1090.

Muñiz-Villareal MS, Manzano-Ramírez A, Sampieri-Bulbarela S et al. (2011) The effect of temperature on the geopolymerization process of a metakaolin-based geopolymer. *Materials Letters* **65(6)**: 995–998.

Najafi Kani E and Allahverdi A (2011) Investigating shrinkage changes of natural pozzolan based geopolymer cement paste. *Iranian Journal of Materials Science and Engineering* **8(3)**: 50–60.

Advances in Cement Research
Volume 28 Issue 1

Temperature rise and initial shrinkage of
alkali-activated fly ash cement pastes
Shekhovtsova, Kovtun and Kearsley

Palomo A, Grutzeck MW and Blanco MT (1999) Alkali-activated
fly ashes: a cement for the future. *Cement and Concrete
Research* **29(8)**: 1323–1329.

Papa E, Medri V, Landi E, Ballarin B and Miccio F (2014)
Production and characterization of geopolymers based on
mixed compositions of metakaolin and coal ashes.
Materials and Design **56**: 409–415.

Provis JL (2009) Activating solution chemistry for geopolymers.
In *Geopolymers. Structure, Processing, Properties
and Industrial Application* (Provis JL and van Deventer
JSJ (eds)). Woodhead Publishing, Cambridge, UK,
pp. 50–71.

Provis JL (2013) Geopolymers and other alkali-activated
materials: why, how and what? *Materials and Structures*
47(1–2): 11–25.

Puertas F, Martínez-Ramírez S, Alonso S and Vázquez T (2000)
Alkali-activated fly ash/slag cements: strength behavior
and hydration products. *Cement and Concrete Research*
30(10): 1625–1632.

Ridtirud C, Chindaprasirt P and Pimraksa K (2011) Factors
affecting the shrinkage of fly ash geopolymers.
*International Journal of Minerals, Metallurgy and
Materials* **18(1)**: 100–104.

Shekhovtsova J, Kearsley EP and Kovtun M (2014) Effect of
activator dosage, water-to-binder-solids ratio, temperature
and duration of elevated temperature curing on the
compressive strength of alkali-activated fly ash cement
pastes. *Journal of the South African Institution of Civil
Engineering* **56(3)**: 44–52.

Škvára F, Šlosar J, Bohunek J and Marková A (2003) Alkali-
activated fly ash geopolymeric materials. In *Proceedings of
11th International Congress on the Chemistry of Cement:
Cement's Contribution to the Development in the
21st Century, Durban, South Africa* (Grieve G and Owens
G (eds)) Durban, South Africa, pp. 1341–1350, CD-ROM.

Somna K, Jaturapitakkul C, Kajitvichyanukul P and Chindaprasirt
P (2011) NaOH-activated ground fly ash geopolymer
cured at ambient temperature. *Fuel* **90(6)**: 2118–2124.

Steveson M and Sagoe-Crentsil K (2005) Relationships between
composition, structure and strength of inorganic polymers.
Part 2 fly ash-derived inorganic polymers. *Journal of
Materials Science* **40(16)**: 4227–4259.

Sukmak P, Horpibulsuk S and Shen SL (2013) Strength
development in clay-fly ash geopolymer. *Construction and
Building Materials* **40**: 566–574.

Tarasov AS, Kearsley EP, Kolomatskiy AS and Mostert HF (2010)
Heat evolution due to cement hydration in foamed
concrete. *Magazine of Concrete Research* **62(12)**: 895–906.

Turner LK and Collins FG (2013) Carbon dioxide equivalent
(CO_2-e) emissions: a comparison between geopolymer
and OPC cement concrete. *Construction and Building
Materials* **43**: 125–130.

Van Deventer JSJ, Provis JL, Duxson P and Brice DG (2010)
Chemical research and climate change as drivers in the
commercial adoption of alkali activated materials.
Waste and Biomass Valorization **1(1)**: 145–155.

Van Jaarsveld JGS and van Deventer JSJ (1999) Effect of the
alkali metal activator on the properties of fly ash-based
geopolymers. *Industrial and Engineering Chemistry
Research* **38(10)**: 3932–3941.

Winnefeld F, Leemann A, Lucuk M, Svoboda P and Neuroth M
(2010) Assessment of phase formation in alkali activated
low and high calcium fly ashes in building materials.
Construction and Building Materials **24(6)**: 1086–1093.

Yang KH, Song JK and Song KI (2013) Assessment of CO_2
reduction of alkali-activated concrete. *Journal of Cleaner
Production* **39**: 265–272.

Zhang Z, Wang H, Provis JL *et al.* (2012) Quantitative kinetic
and structural analysis of geopolymers. Part 1. The
activation of metakaolin with sodium hydroxide.
Thermochimica Acta **539**: 23–33.

Zhang Z, Provis JL, Wang H, Bullen F and Reid A (2013)
Quantitative kinetic and structural analysis of
geopolymers. Part 2. Thermodynamics of sodium silicate
activation of metakaolin. *Thermochimica Acta* **565**:
163–171.

WHAT DO YOU THINK?

To discuss this paper, please submit up to 500 words to
the editor at journals@ice.org.uk. Your contribution will
be forwarded to the author(s) for a reply and, if
considered appropriate by the editorial panel, will be
published as a discussion in a future issue of the journal.